Journal of Machine Engineering, 2019, Vol. 19, No. 2, 63–72
ISSN 1895-7595 (Print) ISSN 2391-8071 (Online)

Received: *07 January 2019* / Accepted: *16 April 2019* / Published online: *29 June 2019*

cemented carbide cutting tools,
titanium aluminides, specific cutting forces,
high feed machining

Daniel FINKELDEI[1*]
Friedrich BLEICHER[1]

END MILLING OF Ti-48Al-2Cr-2Nb UNDER HIGH-FEED CONDITIONS

Gamma titanium aluminides are fast developing materials and particularly in use for aerospace and automotive components. Due to the high cutting forces and raised cutting temperatures achieved during milling of this material, tool-wear is a crucial factor. Thus, increasing of the cutting speed leads to a significant rise of the cutting temperature. On the one hand, the implementation of innovative cooling strategies can reduce the heat flux in the cutting tool. On the other hand, analysing of the heat generation during the cutting process can lead to improved machining strategies. Previous research attempts assess microstructural and chip formation, as well as tool-wear in finish milling of this material. However, few have investigated the optimal cutting strategies in roughing and finishing of titanium aluminides. In this study, the milling operation under high feed rate should be investigated and the potential to improve chip removal rate and tool life should be determined.

1. INTRODUCTION

The automotive and aerospace industry require materials to reduce the weight of their products [1]. Especially titanium aluminides are predestined as a substitution material for heavy-weight nickel based alloys, like Inconel 718. Their high specific strength (high tensile strength at low density) is the main advantage [1]. Furthermore, titanium reacts instantly with oxygen to a protecting surface layer of TiO_2. This passivated surface layer slow down corrosion and oxidation processes. The biggest disadvantage is the high cost of titanium aluminides. There are only a few applications for this group of material. In the automotive industry, Mitsubishi constructed one of the first supercharger engines with a turbine blade completely made of a titanium aluminide alloy [2]. Great development potential can be seen in aerospace engines or gas turbines [3–5]. High temperatures exist in and around the combustion stage where nickel based alloys can show their excellent material behaviour. Different kind of titanium alloys are developed and engineered for this application. In this way, Hadi et al. developed a titanium aluminide with high tensile strength in elevated temperature conditions [5].

[1] TU Wien, Institute of Production Engineering and Photonic Technologies (IFT), Wien, Austria
[*] E-mail: finkeldei@ift.at
https://doi.org/10.5604/01.3001.0013.2224

However, these material properties make it difficult-to-cut [6]. Low material removal rates and less tool-life result in machining of this group of material. The planning of an efficient machining process with high surface quality requires a well-engineered machining strategy. On the one hand, there must be the correct choice of the tool substrate and coating. Titanium has a high chemical affinity [7, 8] to many alternative tool substrates, for example cubic boron nitride and ceramics. Cemented carbide is the best developed tool substrate, particularly they are used in industrial processes [9]. The use of a tool coating depends on the coating material itself if this material gets into chemical reaction with the titanium aluminide; the choice of the correct cooling strategy can help to get better tool life [10].

On the other hand, machining parameters must be set in a correct way. Low thermal conductivity of the material leads to a strong heating of the cutting tool edge when machining with high cutting speeds. Because of this, a targeted cooling strategy has to be installed to dissipate cutting temperature from the cutting edge and to protect the cutting tool from massive tool wear. But high stresses of the machining process require to adjust the cooling strategy for a minimum of tool internal stresses. Another machining strategy is the high performance cutting, where less investigations have been made yet [11].

Nieslony et al. depicted for a (α+β) titanium alloy Ti-6Al-4V that an increase in the undeformed chip thickness results in a decrease of the specific cutting energy [12]. In comparison to the research of Nieslony et al. [12], the decrease of the resulted cutting force in the end milling process of Ti-48Al-2Cr-2Nb should be obtained. The main topic of this article is to describe the potential of high feed machining for this intermetallic titanium aluminide. The investigation should promote the use of this machining strategy to protect the integrity of the cutting edge and to increase the machining performance.

2. EXPERIMENTAL WORK

The characterisation of the specific cutting forces was performed on a turning lathe HEID FS300. All experimental work in the end milling of Ti-48Al-2Cr-2Nb were processed on a machining centre Hermle C20U and C42U. Both machine tools have comparable structures and show a stable machining behaviour. The cutting tests are realized in a linear trimming process. A Kistler 9170A collet chuck tool holder combined with a force measurement system is used for measuring the cutting forces directly at the end milling tool. Measuring of tool wear is realised on a high-speed microscope Keyence VW-9000 and tool wear itself is determined in three sequential stages (M1, M2 and M3) on the rake and flank face for the maximum wear land criterion $VB_{M1..3,max}$ (shown in Fig. 1). In particular for abrasive tool wear VB_{max} is the characteristic wear mechanism; tool notch wear VB_{notch} can be detected after longer machining times over 30 min.

The first end milling process is performed with a five-fluted cemented carbide tool on the machining centre Hermle C42U. The parameter setting is set to a cutting speed $v_c = 40\ \mathrm{m \cdot min^{-1}}$, feed $f_z = 0.05\ \mathrm{mm \cdot tooth^{-1}}$ as well as a radial and axial depth of cut $a_e = 4$ mm and $a_p = 10$ mm. The process is supported by flood cooling with a volume flow rate of $20\ \mathrm{L \cdot min^{-1}}$.

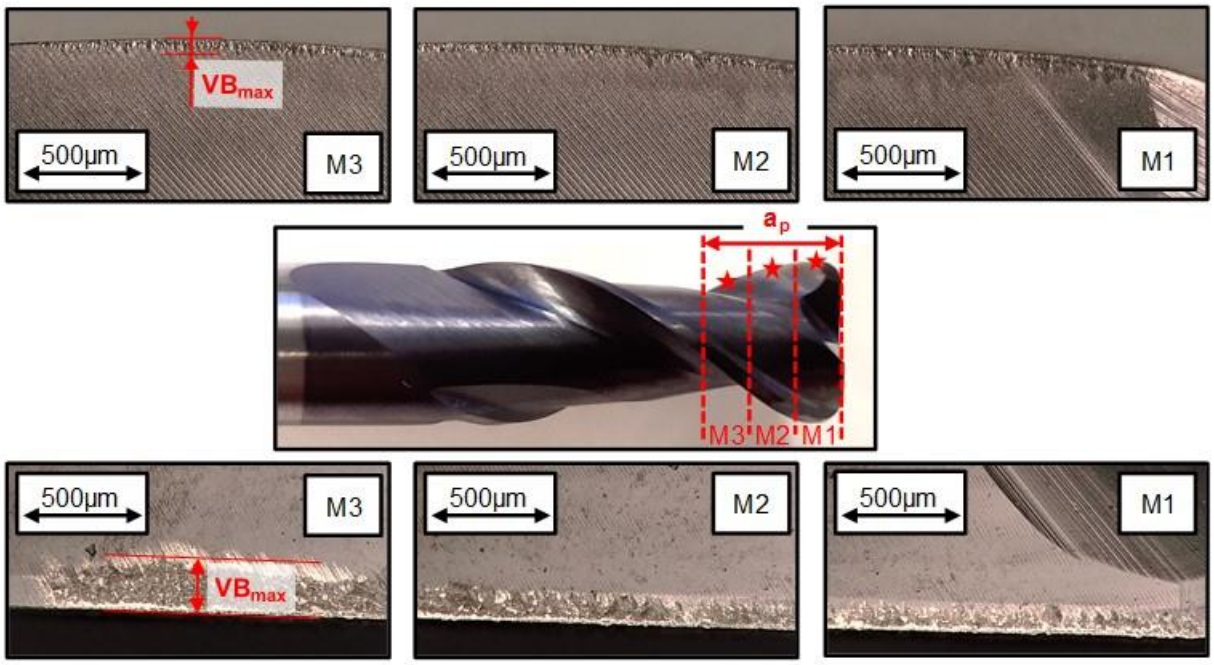

Fig. 1. Declaration for the measurement of tool wear; shown schematically for the two-fluted cutting tool

The second end milling process is machined with a prototype cutting tool (shown in Fig. 2b) on the machining centre Hermle C20U for the high performance cutting (HPC) process. The geometrical properties are published in Fig. 2c. A cutting speed $v_c = 30\ \mathrm{m \cdot min^{-1}}$ as well as a radial and axial depth of cut $a_e = 2$ mm and $a_p = 5$ mm has been chosen. Feed has been variated in three stages of $f_z = \{0.05,\ 0.075,\ 0.1\}\ \mathrm{mm \cdot tooth^{-1}}$, which are initial feed conditions to determine higher feed behaviour in machining of this intermetallic titanium aluminides. The cooling system is flood cooling with only one difference: Coolant is supplied through the collet chuck of the tool holder but not through the cutting tool itself (shown in Fig. 2a) with a volume flow rate of $20\ \mathrm{L \cdot min^{-1}}$. Additionally, tool wear of the three feed conditions is compared for constant steps of the material removal V_w.

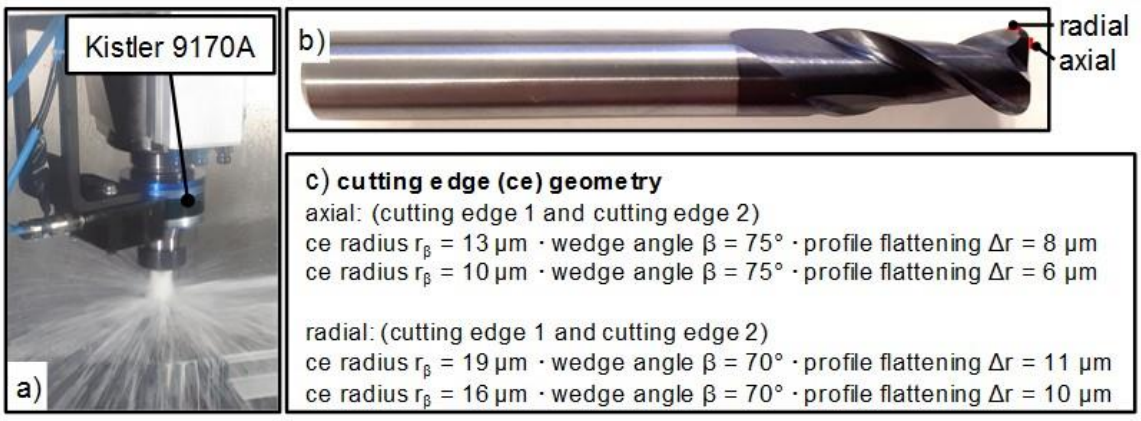

Fig. 2. a) setup of the machining process, b) image of the end mill prototype,
c) geometrical measurement of the end milling prototype

3. MATERIAL CHARACTERISATION OF TI-48AL-2CR-2NB

The high-dynamic material parameter of this type of intermetallic titanium aluminide are determined by a Split Hopkinson pressure bar test and presented in Fig. 3. The experimental setup consists of 15 strain values ranged in an interval of 0.002 to 0.4 and four strain rates ranged in an interval of 0.001 to 2000 s^{-1}. Temperature dependence is measured for a strain rate of 200 s^{-1} and four temperature values in a range of 20°C up to 600°C. Based on the material law and measurement data, the machining behaviour was estimated in an analytical way. The Johnson-Cook material law can be used for finite element analysis.

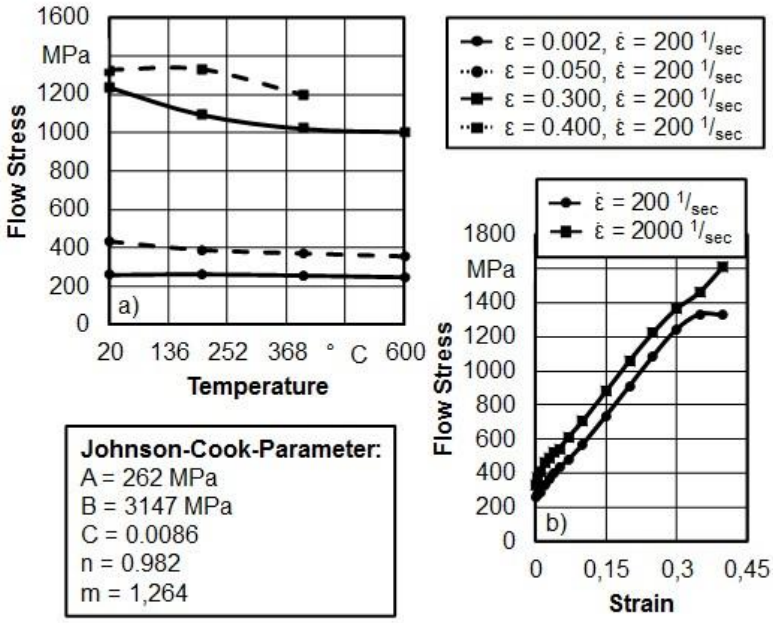

Fig. 3. High dynamic material characterisation and determination of the Johnson-Cook material law of Ti-48Al-2Cr-2Nb

The intermetallic microstructure of titanium aluminides like Ti-48Al-2Cr-2Nb shows a metallic-ceramic material behaviour in deformation processes. This can be seen in the stress-strain curve of Fig. 3a. Furthermore, Ti-48Al-2Cr-2Nb has an interesting behaviour under a deformed status of a high strain rate. Low strain ($\varepsilon = 0.002$) shows no temperature dependent behaviour. Higher strain of $\varepsilon = 0.05$ and $\varepsilon = 0.3$ develop against a steady state stress level in high temperature conditions. However, there can be the typical decrease in the stress-strain curve for higher temperature levels (> 600°C). It is a different material behaviour to metallic steels like nickel based alloys, for example Inconel 718.

The strain rate strengthening of Ti-48Al-2Cr-2Nb increases very slowly, which is legible in the coefficient C of the Johnson-Cook-parameter (Fig. 3). In combination with the higher coefficient m, which is an indicator for the influence of an increased flow stress due to higher workpiece temperatures, and due to the low thermal conductivity, high strain

rates caused by high cutting speeds induce high workpiece and cutting tool temperatures. The elevated heat transfer into the cutting tool weakens the tool substrate and tool failure is significantly accelerated.

Another important material coefficient is the specific cutting force. This coefficient can be predicted by the Kienzle equation and describes the relation between the cutting forces and the pressure at the cutting edge. The equations (1) and (2) show the typical mathematical structure of the Kienzle equation for the prediction of the cutting force and the feed force [13]. Additionally, the calculated values for the specific cutting forces and feed forces are written in Table 1.

$$k_c = k_{c1.1} * h^{-m_c} * {v_c}^{C_1} * \left(1 - \frac{\gamma - 2°}{100}\right)^{C_2} \tag{1}$$

The calculation of the normalized specific cutting forces $k_{c1.1}$ and $k_{f1.1}$ is based on the three factors cutting speed v_c, feed f and rake angle γ. Cutting speed is varied in three steps of {10, 30, 40} $\mathrm{m \cdot min^{-1}}$, feed f is varied in seven steps of {0.03, 0.07, 0.09, 0.15, 0.2, 0.25, 0.3} $\mathrm{mm \cdot rev^{-1}}$ and rake angle is varied in five steps of {0, 5, 10, 15, 20}.

$$k_f = k_{f1.1} * h^{-m_f} * {v_c}^{C_1} * \left(1 - \frac{\gamma - 2°}{100}\right)^{C_2} \tag{2}$$

Both force components show the same characteristic. There are low normalized force coefficients $k_{c1.1}$ and $k_{f1.1}$ as well as high slope factors m_c and m_f. Higher slope factors describe the mathematical behaviour e.g. at low feed (for example $f = 0.03\ \mathrm{mm \cdot rev^{-1}}$) that there is a significant decrease of the specific cutting force k_c for an incrementally increased feed. The proportion of the incremental increase of the feed f and the incremental decrease of the specific cutting force k_c is determining for the development of the resulting cutting force F_c.

Table 1. Coefficients of the specific cutting forces and feed forces

	$k_{1.1}$	m	C_1	C_2
Cutting force F_c	677.90 MPa	0.42	0.096	-0.032
Feed force F_f	162.16 MPa	0.50	0.363	-1.631

The high slope factor of the specific cutting force can be explained by the high dynamic material behaviour and the mechanics of the machining process. As it can be seen in Fig. 3b, deformation of Ti-48Al-2Cr-2Nb causes significant strain hardening of the material. In the machining process, deformation will be generated in the primary shear zone. As much as the microstructure will be deflected, strain raises.

4. END MILLING OF TI-48AL-2CR-2NB WITH CONVENTIONAL MACHINING PARAMETERS

Machining of Ti-48Al-2Cr-2Nb with cemented carbide end milling tools need well-engineered cutting tools. An adequate tool geometry and tool substrate was analysed in a wide-ranged investigation of a previous work. This tool geometry shows an edge radius

which protects the cutting tool in the tool corner. For the machining process depicted in Fig. 4, an edge radius of r_e = 3 mm has been chosen. Moreover, a sharp cutting edge with a minimal cutting edge radius is necessary to cut the material and to secure the tool cutting edge of fast notching. A cutting edge radius of r_β = 10 µm has been evaluated to protect the cutting tool for massive notching.

When adapting the tool geometry according to these constraints, tool-wear progresses slowly. Tool wear land of the rake face reaches approximately 100 µm after a cutting time of 30 min. In comparison to this, flank face only has an insignificant characteristic in this rough end milling process. Both tool wear lands of the flank face and the rake face are depicted in Fig. 5. Furthermore, the cutting force varies around 1450 N, which generates a specific cutting pressure of 4500 MPa with the current machined chip cross section of A = 0.32 mm².

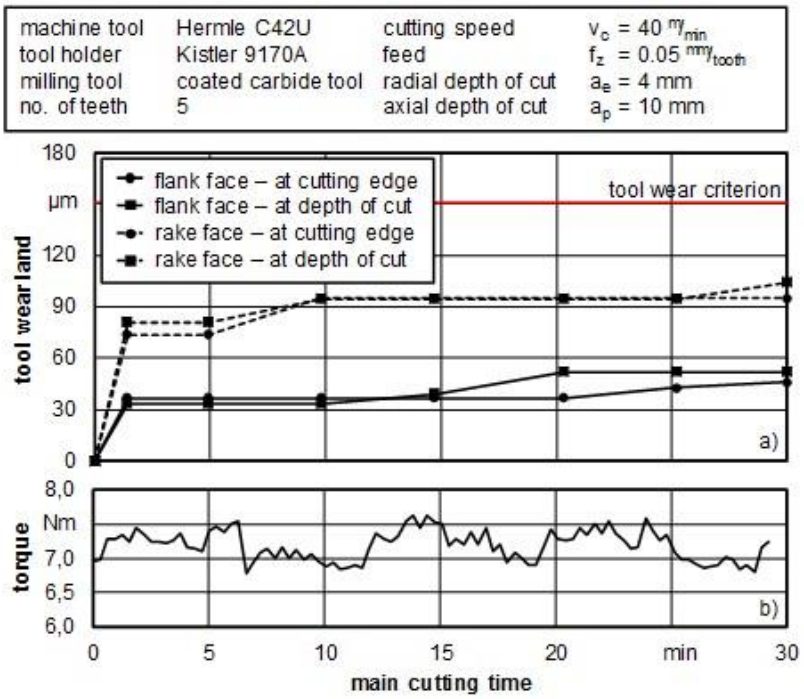

Fig. 4. Tool wear and torque of a carbide cutting tool in trimming of Ti-48Al-2Cr-2Nb

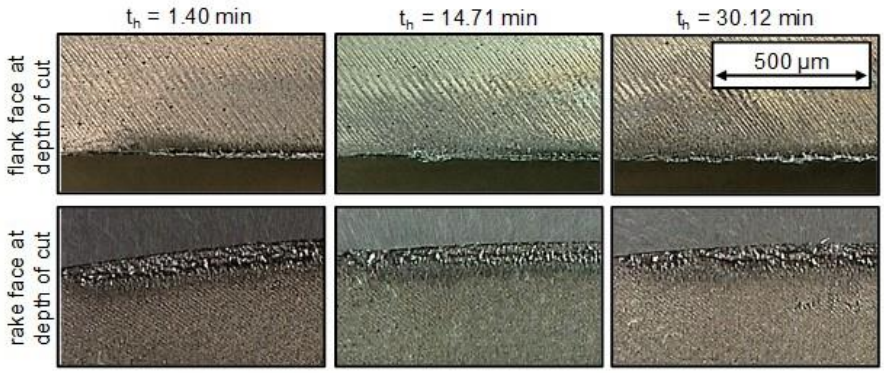

Fig. 5. Tool wear of the flank and rake face of the carbide cutting tool in trimming of Ti-48Al-2Cr-2Nb

This machining configuration is currently one of the best settings to cut Ti-48Al-2Cr-2Nb. Higher cutting speeds need an adjusted process strategy to dissipate the cutting temperature from the cutting tool. Another possible way for increasing the performance of the machining process could be the machining strategy of the high performance cutting (HPC). Referring to the previous Chapter, the influence of increasing feed on the machining behaviour should be investigated. However, to protect the cutting edge of increased tool load when machining at higher feed, the radial and axial depth of cut will be decreased to the half of the above used values. This will decrease cutting forces approximately to the half of its original value. But in calculation of the specific cutting forces, this coefficient will increase with 12% for this new cutting conditions because of the decrease of the radial depth of cut and the undeformed chip thickness.

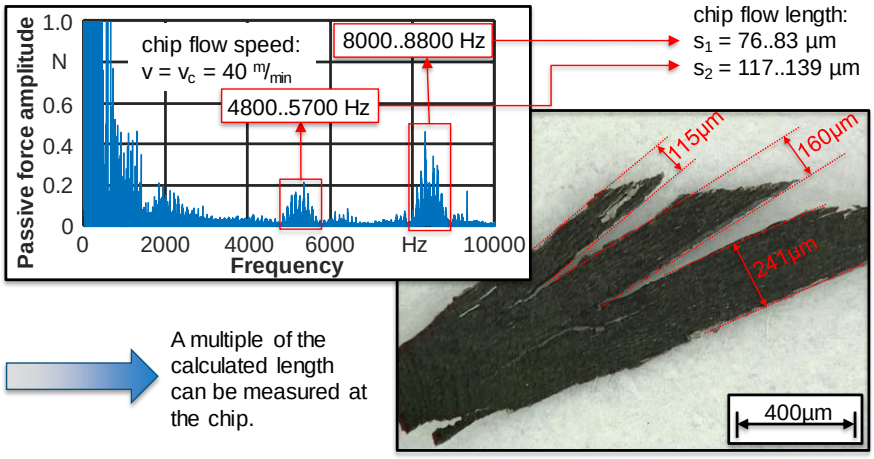

Fig. 6. Analysis of the fragmental chips with recurring segments

End milling of Ti-48Al-2Cr-2Nb causes fragmental chips because of the brittle-hard material behaviour. As it is known from literature, titanium alloys tend to form segmented chips. This is similar to the machining of titanium aluminides which is depicted in literature [11] and Fig. 8. However, there are some characteristic peaks in the frequency analysis of the measured cutting forces which belongs to the recurring cracks of the chip segments.

5. END MILLING OF TI-48AL-2CR-2NB WITH ADVANCED FEED CONDITIONS

Based on the cutting process above, the machining behaviour is analysed for the variation of three feed rates. The standard feed is set to $f_z = 0.05$ mm · tooth^{-1}, while the other ones are determined to $f_z = 0.075$ mm · tooth^{-1} and $f_z = 0.1$ mm · tooth^{-1}. To get a comparable result for the development of tool-wear, the axial depth of cut a_p is fixed to 5 mm. The tool-wear on the flank face, which is published in Fig. 7, shows massive abrasive wear for the cutting tool that is machined with a feed of $f_z = 0.05$ mm · tooth^{-1}. Because of the low radial depth of cut of $a_e = 2$ mm, the mean chip thickness is $h_m = 0.022$ mm.

The cutting edge radius r_β of the cutting tool is 19 µm. The other feed rates have a mean chip thickness of $h_m = 0.034$ mm ($f_z = 0.075$ mm · tooth^{-1}) and $h_m = 0.045$ mm ($f_z = 0.1$ mm · tooth^{-1}). At the increased feeds, the flank faces show less abrasive wear. Only the cutting tool, which machined with the lowest feed rate, shows a small notch wear on the flank face. However, the tool-wear on the flank face (Fig. 7) and rake face (Fig. 8) is insignificant.

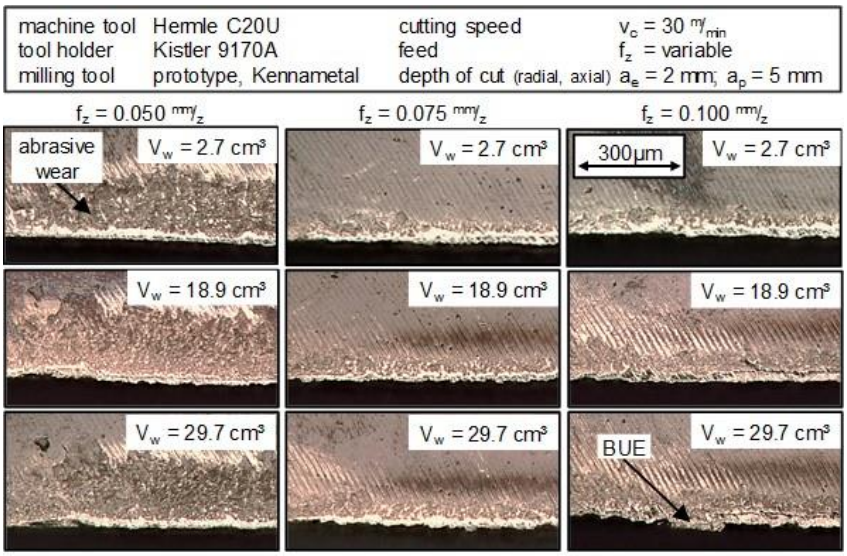

Fig. 7. Tool wear at the flank face of the cutting tool determined for constant steps of the material removal V_w

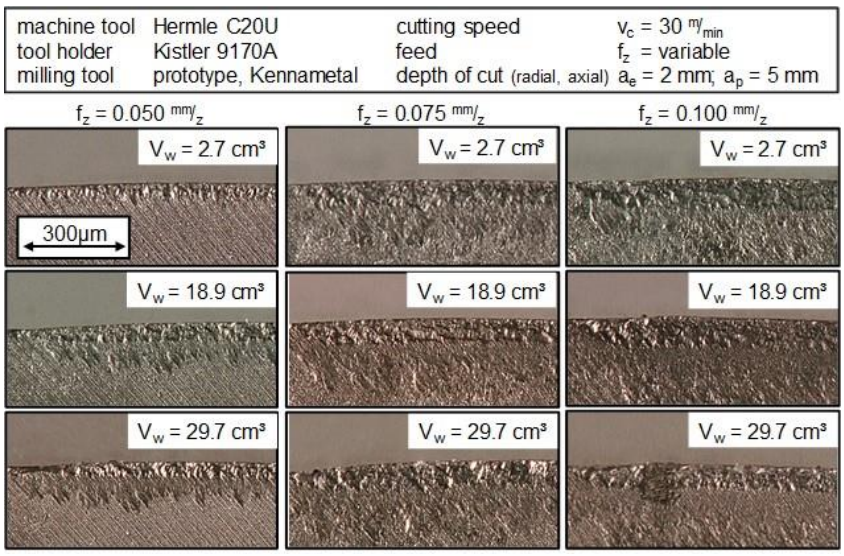

Fig. 8. Tool wear at the rake face of the cutting tool determined for constant steps of the material removal V_w

In milling, torque M_z is proportional to the cutting force F_c. The machining process with the feed of 0.05 mm · tooth^{-1} has a torque of $M_z = 2.32$ Nm, while the second machining process with a feed of 0.075 mm · tooth^{-1} has a torque of $M_z = 3.26$ Nm and the third machining process with a feed of 0.1 mm · tooth^{-1} shows a torque of $M_z = 4.12$ Nm (shown in Fig. 9). However, the fixed axial depth of cut of $a_p = 5$ mm lead to three different chip cross

sections in the machining processes. As a result, there is a linear slope in all of the three torque values. In a further step, the cutting processes with the higher feed rates must be normalised to the chip cross section value of the standard feed rate. The normalisation can be calculated by equation 3 and can be done because of the linear ratio of the axial depth of cut and the cutting force.

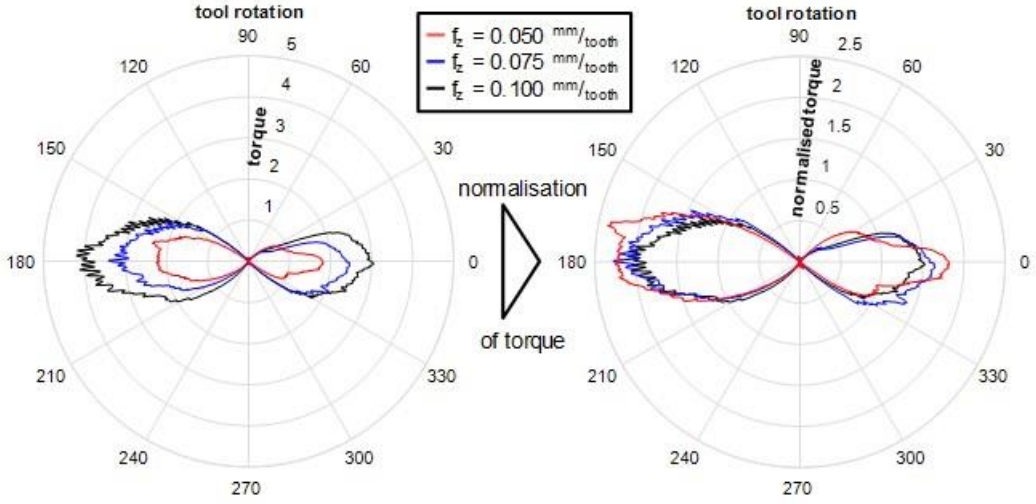

Fig. 9. Torque and normalised torque measured in the trimming process with high performance cutting

$$M_{z,i,\mathrm{norm}} = \frac{A_1}{A_i} * M_{z,i} \text{ , with } i \in \{1,2,3\} \tag{3}$$

The normalised torque values for the three feed rates are $M_{z,1}$ = 2.32 Nm, $M_{z,2}$ = 2.18 Nm and $M_{z,3}$ = 2.06 Nm. A decrease in torque has been measured, which described the statement of Chapter 3 that there is a decrease in cutting forces when increasing the feed rate.

6. CONCLUSION / SUMMARY

The results of this investigation show the potential of the machining process to implement the strategy of high performance cutting (HPC) for the end milling process of the intermetallic titanium aluminide Ti-48Al-2Cr-2Nb. As it was shown in the material behaviour of the specific cutting forces of Ti-48Al-2Cr-2Nb, a low normalised cutting force $k_{c1.1}$ and a high slope factor m_c are determined. Especially the high slope factor describes the mechanism to decrease the resulting cutting forces when increasing feed. This theoretical mechanism was demonstrated in an experiment for a three-staged variation of the feed between $f_{z,1}$ = 0.05 mm · tooth^{-1}, $f_{z,2}$ = 0.075 mm · tooth^{-1} and $f_{z,3}$ = 0.1 mm · tooth^{-1}.

The TU Wien will continue further investigations regarding the end milling with the strategy of the high performance cutting (HPC) of Ti-48Al-2Cr-2Nb. The topic of this research should be the description of this special machining process to get more information

of potentials in improving the machinability of titanium aluminides with conventional end milling tools published in Chapter 4.

ACKNOWLEDGEMENTS

The authors acknowledge Kennametal GmbH in Nuremberg, Germany for providing the two-teethed prototype of the cemented carbide end milling tools used in this investigation. Special thanks also to Mr. Jochen Gross for his technical support.

REFERENCES

[1] CASTELLANOS S.D., CAVALEIRO A.J., JESUS A.M.P.D., NETO R., ALVES J.L., 2019, *Machinability of titanium aluminides : a review*, Journal of Materials: design and applications, 233, 3, 426–451.
[2] CLEMENS H., 2011, *Intermetallisches titanaluminid – ein innovativer leichtbauwerkstoff für hochtemperatur – anwendungen*, BHM, 156, 255–260.
[3] MANTLE A.L., ASPINWALL D.K., 1997, *Surface integrity and fatigue life of turned gamma titanium aluminide*, Journal of Materials Processing Technology, 72, 413–420.
[4] APPEL F., OEHRING M., WAGNER R., 2000, *Novel design concepts for gamma-base titanium aluminide alloys*, Intermetallics, 8, 1283–1312.
[5] HADI M., MERATIAN M., SHAFYEI A., 2015, *The effect of lanthanum on the microstructure and high temperature mechanical properties of a beta-solidifying TiAl alloy*, Journal of Alloys and Compounds, 618, 27–32.
[6] KOLAHDOUZ S., HADI M., AREZOO B., ZAMANI S., 2015, *Investigation of surface integrity in high speed milling of gamma titanium aluminide under dry and minimum quantity lubricant conditions*, Procedia CIRP, 26, 367–372.
[7] RAHMAN M., WONG Y.S., ZAREENA A.R., 2003, *Machinability of titanium alloys*, JSME International Journal Series C, 107–115.
[8] M'SAOUBI R., OUTEIRO J.C., CHANDRASEKARAN H.,. DILLON JR. O.W., JAWAHIR I.S., 2008, *A review of surface integrity in machining and its impact on functional performance and life of machined products*, International Journal of Sustainable Manufacturing, 1, 1/2, 203.
[9] PRIARONE P.C., KLOCKE F., FAGA M.G., LUNG D., SETTINERI L., 2016, *Tool life and surface integrity when turning titanium aluminides with pcd tools under conventional wet cutting and cryogenic cooling*, International Journal of Advanced Manufacturing Technology, 85, 807–816.
[10] FINKELDEI D., BLEICHER F., 2016, *Investigation of coolants in machining of titanium aluminides*, DAAAM International Symposium, 26, 0825–0833.
[11] KLOCKE F., SETTINERI L., LUNG D., PRIARONE C.P., ARFT M., 2013, *High performance cutting of gamma titanium aluminides: influence of lubricoolant strategy on tool wear and surface integrity*, Wear, 302/1–2, 1136–1144.
[12] NIESLONY P., GRZESIK W., BARTOSZUK M., HABRAT W., 2016, *Analysis of mechanical characteristics of face milling process of ti6al4v alloy using experimental and simulation data*, Journal of Machine Engineering, 16/3, 58–66.
[13] TOENSHOFF H.K., DENKENA B., 2013, *Basics of cutting and abrasive processes*. Berlin, Heidelberg, Springer.